CHARACTERIZATION OF TESSELLATED BISTABLE COMPOSITE LAMINATES

Yuefeng Cui[a], Matthew Santer[a,*]

[a]*Department of Aeronautics, Imperial College London, London, SW7 2AZ, UK*

Abstract

Tessellated surfaces consisting of both unsymmetric composite elements with opposite layups, and unsymmetric composite elements in combination with symmetric composite elements, are investigated. It is shown that in simple cases these continuous surfaces only exhibit bistability due to the strong interaction between the connected elements. Strategies to mitigate against this interaction are proposed and implemented to achieve surfaces with high degrees of multistability up to the theoretical maximum.

Keywords:
Multistable surfaces, Bistable Shells, Tessellation

1. Introduction

In this paper we present an investigation into the connection of bistable composite plates to form space-filling multistable surfaces. This extends previous work (Cui (2015)) on the connection of bistable composite plates in series to achieve multistability.

Due to the mismatch of thermal expansion coefficients along fiber directions, it is well known that composite laminates with unsymmetric layups may exhibit two cylindrical shape at room temperature (Hyer (1981a, 1982)). In addition, the two distinct configurations can transition between each other via a simple actuation. This mechanical behaviour of unsymmetric composite laminates has prompted much research interest, and a number of published works have investigated the bistability of unsymmetric composite laminates (Dang (1986); Jun (1992); Peeters (1996); Dano (1996); Etches (2009)).

Adaptive structures which can change shape to be optimal in various environments are widely demanded for aerospace applications. Multistable com-

*Corresponding author.
Address: South Kensington Campus, London SW7 2AZ, UK, Tel.: +44(0)20 7594 5117
Email address: m.santer@imperial.ac.uk (Matthew Santer)

posites offer such adaptive capability. Conventional adaptive mechanisms require external energy to maintain a new shape after morphing. In contrast, for a multistable structure, energy is only required to be imparted during the actuation process. This represents a great advantage when an adaptive structure is designed to operate in a low energy budget application environment such as, for example, is typically found in space.

When bistable composite laminates are designed for adaptive applications, it is unlikely that a single bistable shell will be sufficient to fulfil a particular function. Either structures possessing a high degree of multistability are needed to provide high levels of reconfigurability, or at the very least bistable shells have to be fixed with other components. Several designs of compound composite structures have been published in the last decade Mattioni (2008); Arrieta (2014); Dai (2013), although none of them achieve a *continuous* composite surface presenting a high degree of multistability.

Continuous multistable composite surfaces were introduced by by Potter (2004) in which localized variation of layup is shown to generate plates with numerous geometrically stable configurations. They present an analysis of the effect of internal stresses on the presence of regional distortions and stable states and note that, in principle, the potential for unlimited stable states exists. Based on this work Eckstein (2012) hypothesizes the square regions could be locally snapped through to generate multistable "checkerboard" surfaces. Examples of such surfaces, discretized into rectangular regions, are presented in Panesar (2012) in which zero-order design optimization is used to generate tow-steered bistable plates for morphing aerospace applications. The resulting structures are bistable as desired but are observed to exhibit intermediate stable configurations which are not subjected to further investigation.

Detailed investigation into the interaction between adjacent discrete bistable regions was carried out by Cui (2015); in this study highly multistable composite surfaces are achieved by series-connected identical composite shells. Three coupled bistable composite shells with tailored asymmetric bistability demonstrated a maximum of seven stable shapes. This investigation demonstrates that, in principle, a multistable surface consisting of bistable plates connected in series can be extended indefinitely with n connected units resulting in a multistable system with 2^n discrete stable states.

Building on this work, this paper introduces an investigation of novel multistable tessellated composite surfaces which have both high levels of multistability and which, crucially, fill space in two dimensions. We consider cases when the individual bistable elements form a two-dimensional checkerboard shape surface: tessellated surfaces consisting of a maximum of nine bistable square composite units are introduced. To avoid the behaviour of these compound surfaces replicating that of a large single bistable composite shell, each

individual composite element must be distinct from all adjacent elements. The surfaces are composed of composite shells with opposite unsymmetric layups or symmetric composite shells. This therefore first necessitates an investigation of a surface composed of two bistable composite shells with opposite layups. The response of this structure will be use to interpret the behaviour of the subsequently investigated tessellated surfaces. Simulation of the surfaces is carried out using the commercial finite element software *Samcef* v13.1 which enables assessment of the surface behaviour and a qualitative understanding of the underlying phenomenon. The predicted behaviour is verified by comparison with experimental models.

The goal of this paper is the creation of a space filling, continuous multistable structure having n connected bistable sub-elements, which exhibit the theoretically maximum 2^n discrete stable configurations. This is successfully achieved. Additionally it is intended to gain a strong qualitative understanding of the interactions between coupled bistable units on the achievable degree of multistability.

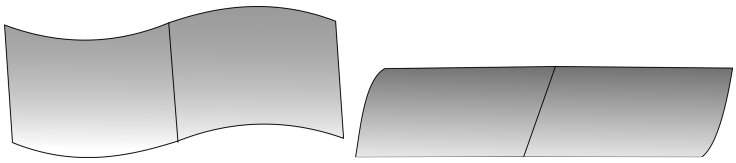
2. Connected bistable shells with opposite layups

As a tessellated surface consisting of unsymmetric composite shells with opposite layups will be investigated in this work, the behaviour of the fundamental unit — two connected composite shells with opposite layups — is considered first. The shells are fabricated from *Hexcel* $IM7-8552$ Graphite/Epoxy Prepreg. The mechanical properties are taken from the manufacturer's data sheet and are listed in Table 1. To ensure the curved shells demonstrate a moderate out-of-plane displacement, the side length of the square laminate is set as 100 mm and the two composite shells are made with unsymmetric stacking sequences [0/90] and [90/0] respectively. For ease of identification of different configurations, we use a binary notation to represent the states following and extending the practice introduced by Cui (2015). If a shell has principal nonzero curvature perpendicular to the linking edge, the shell is defined as being in state 0; otherwise, it is in state 1. In addition, to distinguish the two different composite shells, the states of a shell with [90/0] layup are denoted $\bar{0}$ and $\bar{1}$.

Table 1: Properties of IM7/8552 carbon fibre UD lamina

E_{11} (GPa)	E_{22} (GPa)	G_{12} (GPa)	ν_{12}	α_1 ($10^{-6}/°C$)	α_2 ($10^{-6}/°C$)	thickness (mm)
164	12	5.3	0.33	-0.02	31.2	0.131

When two identical bistable composite shells are connected along common edges the resulting compound surface is shown to exhibit two stable configurations in which the two bistable elements are curved along the same direction Cui (2015). These two states are denoted primary states 00 and 11 respectively. According to the Extended Classic Lamination Theory (ECLT) (Hyer (1981b)), two bistable composite shells with opposite layups would exhibit the same curvature but opposite sign when they are in the same state. In primary state $1\bar{1}$, both shells have nonzero principal curvatures of opposite sign perpendicular to the straight linking edge. As no additional strain energy is introduced, the state is therefore necessarily stable as illustrated in Fig. 1a. In primary state $0\bar{0}$, the two linking edges have the same curvature but with opposite sign. To achieve a connection along the full edge, the two shells have to be subject to significant deformation as shown in Fig. 1b. The induced strain energy may be large enough to actuate the potentially stable shells. Except for the two primary states, the compound surface has two intermediate states $0\bar{1}$ and $1\bar{0}$ which are shown in Fig. 2. To understand the behaviour of this surface, the stability of the four states needs to be investigated.



(a) State $1\bar{1}$ (b) State $0\bar{0}$

Figure 1: Primary state $1\bar{1}$ and $0\bar{0}$ configurations of coupled composite shells with opposite layups [0/90] and [90/0]

Finite element analysis is used to predict the stability of these states. Following the numerical analysis and actuation strategy detailed in Cui (2015), a single square composite shell is meshed with 400 8-node square elements which is shown to provide mess-independent results. A geometrically nonlinear static analysis strategy is applied. After thermal curing, the coupled composite shells with opposite layups are initially in stable state $1\bar{1}$. This means the state $1\bar{1}$ is the preferred stable state. Next, one shell is actuated by means of displacement control with the other shell fixed. This actuation is simulated by holding the four corners of the unactuated shell fixed and displacing the nodes of the actuated shell into an approximation of the snapped-through configuration. At this point all boundary conditions, with the exception of full fixation at a single arbitrary point to prevent rigid body motion, are released to allow the system to adopt an energetically-preferential state. The compound surface reaches the intermediate state $0\bar{1}$. It is observed that the driven shell does not

automatically snap through after the displacement control is released. This demonstrates the intermediate state $0\bar{1}$ is a stable state. Due to symmetry, the stability of intermediate state $1\bar{0}$ may be directly inferred. Fig. 2 illustrates the configurations of the two composite shells in the state $0\bar{1}$ and their corresponding strain energy. In the figure 100% relative actuation indicates the bistable shell is fully actuated. It is clear that neither of the shells reaches the strain energy peak in the intermediate state and the whole structure is at a local potential energy minimum as shown in Fig. 3. This is because these two composite shells curve towards the same direction in the intermediate state. The interaction between the shells is therefore relatively weak. Both of the shells would not be actuated to the other state by the induced strain energy. This is a general result — if two or more adjacent bistable elements are connected in such a way that zero, or minimal, deformation is induced the compound structure will itself be stable.

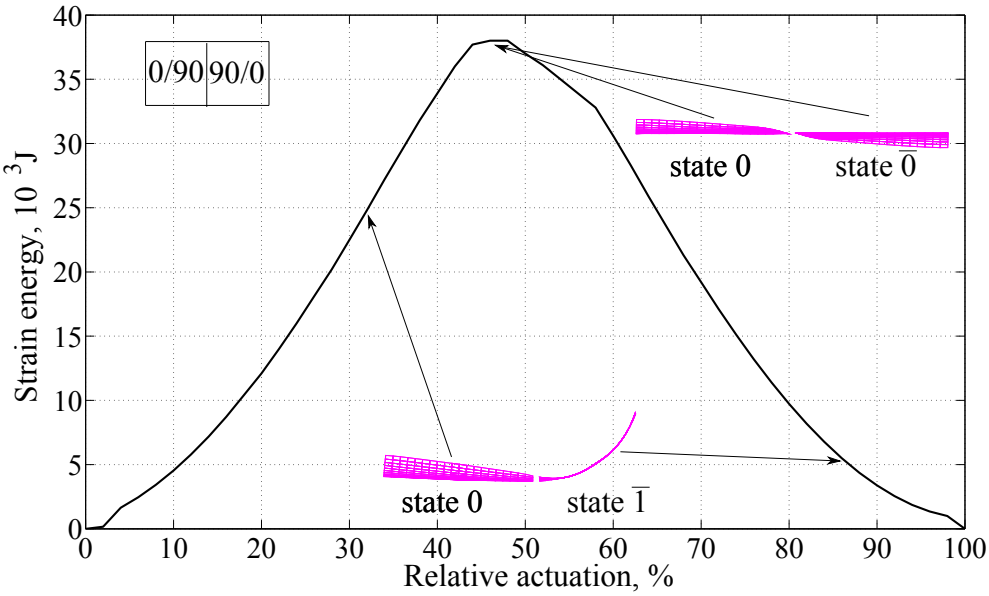


Figure 2: Configurations of two bistable shells with opposite layups [0/90] and [90/0] and their corresponding strain energy levels

Having studied the stability of two intermediate states and one primary state, the connected bistable shells are transitioned to the other primary state $0\bar{0}$. Fig. 2 shows the configurations of both composite shells and their corresponding strain energy. In this case the originally curved linking edges of the shells are deformed such that they are straight. These deformations introduce sufficient energy to actuate the shells and consequently the primary state $0\bar{0}$ of this compound surface is not stable.

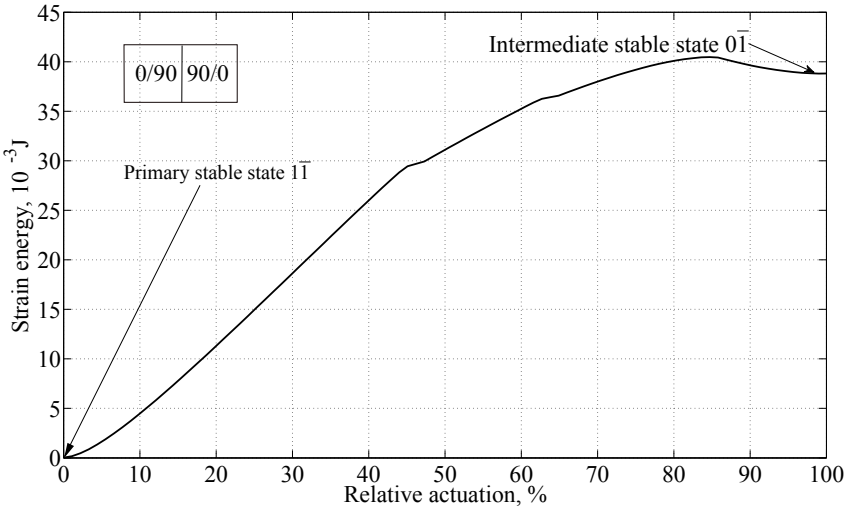
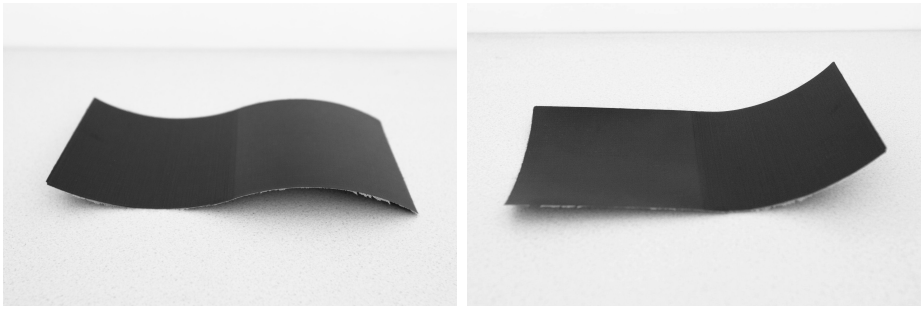


Figure 3: Strain energy vs. relative actuation displacement percentage plots for coupled bistable composite shells with opposite layups

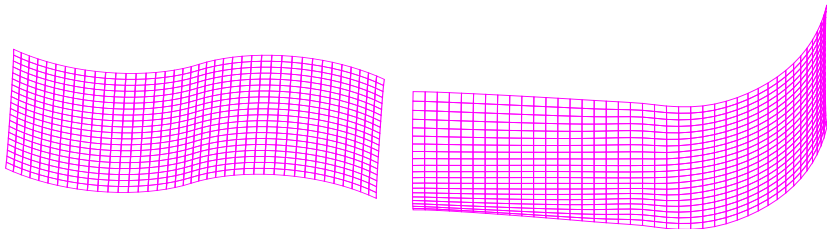
This coupled bistable composite shell with opposite layups is manufactured to verify the FE results. Fig. 4 shows the comparison of FEA predictions and the experimental results. The first primary state $1\bar{1}$ shows close qualitative agreement. In the intermediate stable state $0\bar{1}$, the numerically-predicted shape of the compound shell presents a larger out-of-plane displacement. The results are qualitiatively similar and it it is believed that the minor differences in geometry are the result of manufacturing error and thickness variation. However, the qualitative agreement is sufficient to validate the results so the discrepancies are not subjected to further investigation. The real compound surface is found, as predicted, to exhibit three stable states: the primary state $0\bar{0}$ is not stable.

3. Tessellated bistable composite shells

Having understood the behaviour of the surface consisting of two bistable composite shells with opposite layups, we are now in a position to investigate the behaviour of larger square surfaces. This paper focuses initially on tessellated surfaces composed of 3×3 shells. The first test case introduced is made of composite shells with opposite layups as shown in Fig. 5. Theoretically, a structure composed of bistable elements may demonstrate high degree of multistability. However, the restrictions imposed by linking edges can affect the bistable behaviour of composite elements and the multistability of the whole surface. The side length of each square element is selected to be 50 mm.



(a) Primary state $1\bar{1}$ (b) Intermediate state $0\bar{1}$



(c) Primary state $1\bar{1}$ (FEA) (d) Intermediate state $0\bar{1}$ (FEA)

Figure 4: Coupled square shells ([0/90] and [90/0]) demonstrating tristable behavior. The stability of state $1\bar{0}$ is inferred by symmetry.

0/90	90/0	0/90
90/0	0/90	90/0
0/90	90/0	0/90

Figure 5: Tessellated surface test case 1

Fig. 6 shows the stable configuration of the surface designated test case 1. This surface presents an undulating shape, and the out-of-plane displacement is relatively small throughout the surface. If the unconstrained shape of an element with [0/90] layup has non-zero principle curvature along the $x-$axis, the element is defined as being state 0; otherwise, it is in state 1. The states of a element with [90/0] layup are denoted $\bar{0}$ and $\bar{1}$. Thus, the state of test case 1 can be denoted as follows:

$$\begin{matrix} 0 & \bar{1} & 0 \\ \bar{1} & 0 & \bar{1} \\ 0 & \bar{1} & 0 \end{matrix}$$

Except for the initial stable state, following a similar procedure to that described in the previous section only one more stable configuration of this compound surface is found to exist:

$$\begin{matrix} 1 & \bar{0} & 1 \\ \bar{0} & 1 & \bar{0} \\ 1 & \bar{0} & 1 \end{matrix}$$

The stable configurations of this compound surface are verified by the behaviour of a physical model. The cured composite surface demonstrates only two symmetric stable states. Only one of the stable states is shown in Fig. 7. It is clear that a good qualitative agreement between prediction and reality is achieved.

In this compound surface design, every bistable element has to be connected with two or more bistable elements with opposite layups. The strong interactions largely limit the movement of these bistable elements. As mentioned in the study of coupled distinct bistable shells in the last section, an individual bistable unit is not stable when both adjacent elements are in state 0. Consequently, when one element is actuated via displacement control upon release, all the other elements will be triggered into a dynamic snapthrough. It is also noted that this surface does not present significant out-of-plane displacements in either of its two stable configurations. Therefore, the applicability of these configurations to practical adaptive applications is considered small.

As the first test case does not achieve multistability, a second test case – designated test case 2 – is considered as shown in Fig. 8, in which all [90/0] composite elements are replaced by monostable symmetric elements. This follows the work of Mattioni (2008). According to Mattioni's results, a bistable composite shell can retain bistability when one edge is constrained by a monostable shell. The connection will lead the curvature parallel to the linking edge to be significantly reduced, while the effect on the curvature perpendicular to the linking edge is limited.

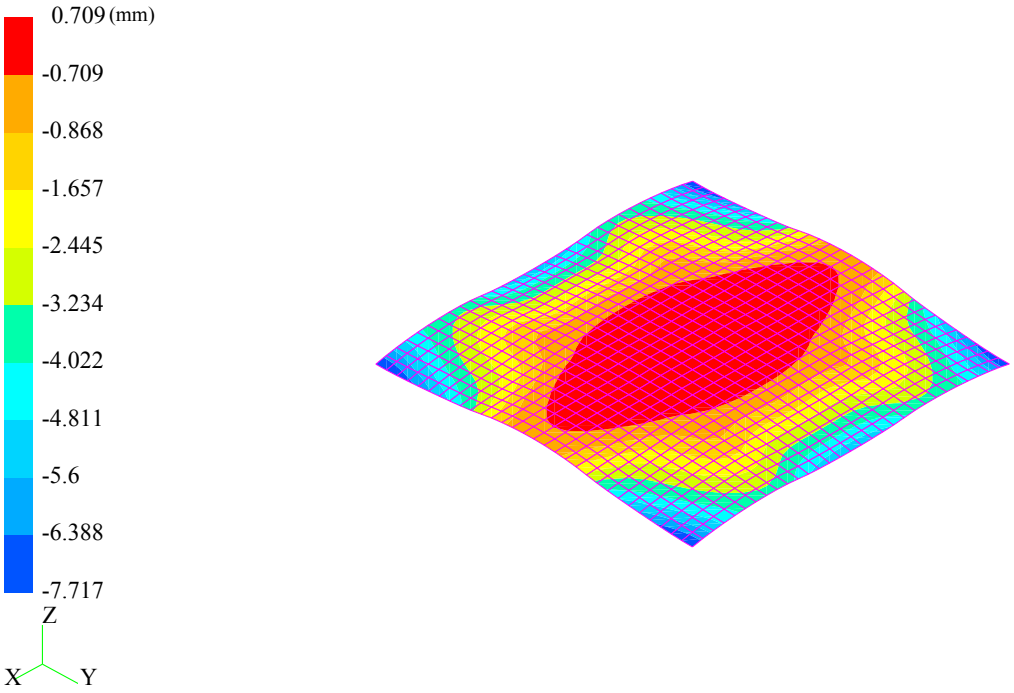


Figure 6: FEA result of a stable configuration of test case 1. The contours indicate positive displacement in the z-axis.

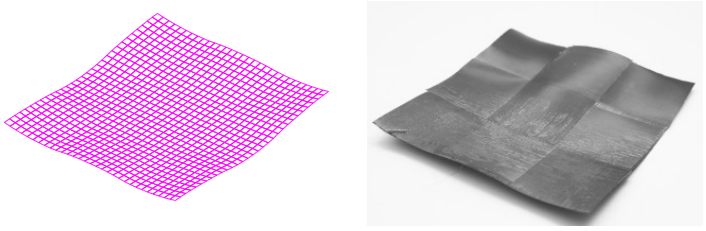


Figure 7: A stable configuration of a physical model of test case 1 and the corresponding FEA result

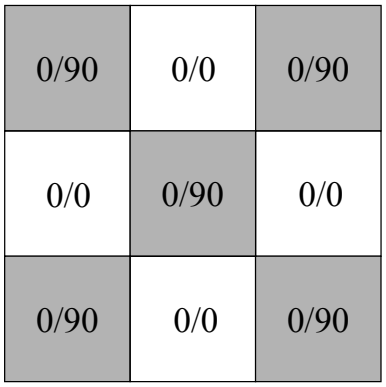


Figure 8: Tessellated surface test case 2

Fig. 9 illustrates the initial stable shape of the compound surface of test case 2. This stable state is denoted

$$\begin{matrix} 1 & s & 1 \\ s & 1 & s \\ 1 & s & 1 \end{matrix}$$

in which s represents the symmetric laminates. Compared with the stable configuration of surface in test case 1, this compound surface exhibits larger out-of-plane displacement and a near semi-cylindrical shape. All the bistable elements have principal curvature along the same axis and with the same sign. When the compound surface is in this stable state, each bistable element located at the corner is connected by two monostable shells. Their curved edges are constrained by symmetric shells having a fibre direction perpendicular to the linking edges whereas their straight edges are constrained by symmetric shells having fiber direction parallel to the linking edges. Since the symmetric composite elements are orthotropic and exhibit weak stiffness perpendicular to the fiber direction, the curved bistable elements are not subjected to strong interactions. Furthermore, out-of-plane displacements are introduced through the linking edges to the unsymmetric composite shells which are originally flat. Thus the compound surface presents an approximately cylinderical stable configuration.

To achieve a new stable configuration, displacement-controlled actuation is applied to each of the bistable elements in sequence. All four corners of the central element are fully fixed and the free corners of the bistable element to be actuated are displaced into a geometry close to the free second bistable configuration. However, upon release of these actuating displacements the driven shell is found to dynamically snap back indicating the instability of the

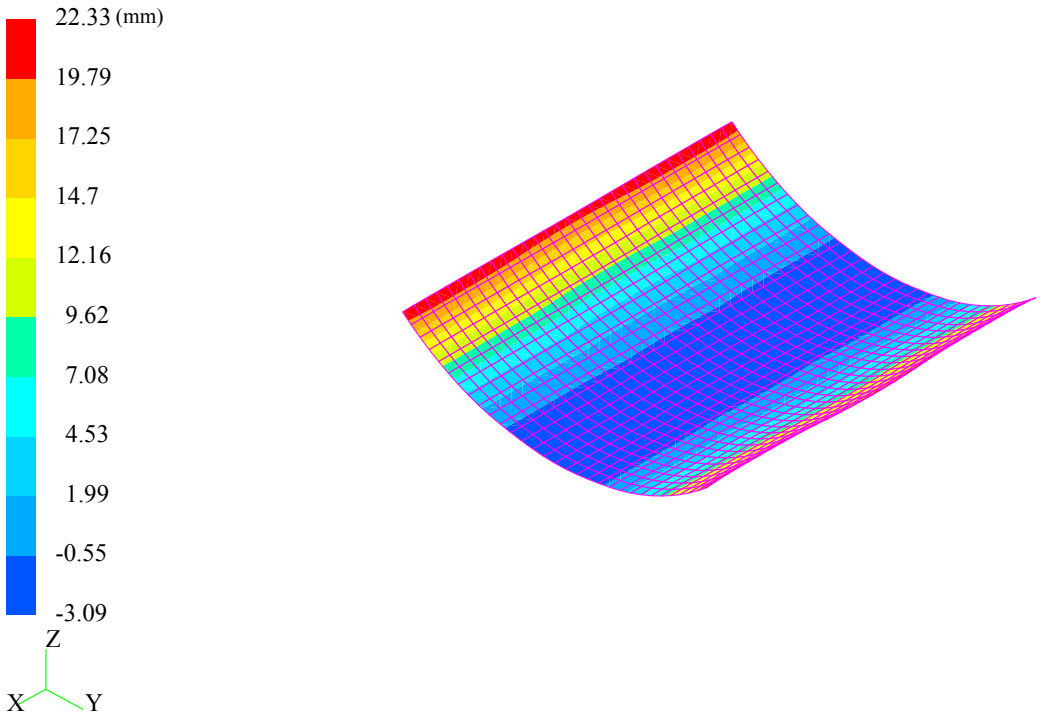


Figure 9: Initial stable configuration of the compound surface of test case 2. The contours indicate positive displacement in the z-axis.

new configuration. The FE results show that no new energy equilibrium can be obtained by actuating any one or two bistable elements individually. When, and only when, all the bistable elements are actuated together, the surface can achieve a new stable configuration, specifically

$$\begin{matrix} 0 & s & 0 \\ s & 0 & s \\ 0 & s & 0 \end{matrix}$$

as shown in Fig. 10. Clearly, the new stable configuration presents less out-of-plane displacement than the initial stable configurations. From the energy graph plotted in Fig. 11, we also notice the strain energy of the second stable state is much higher. The compound surface of test case 2 is therefore bistable.

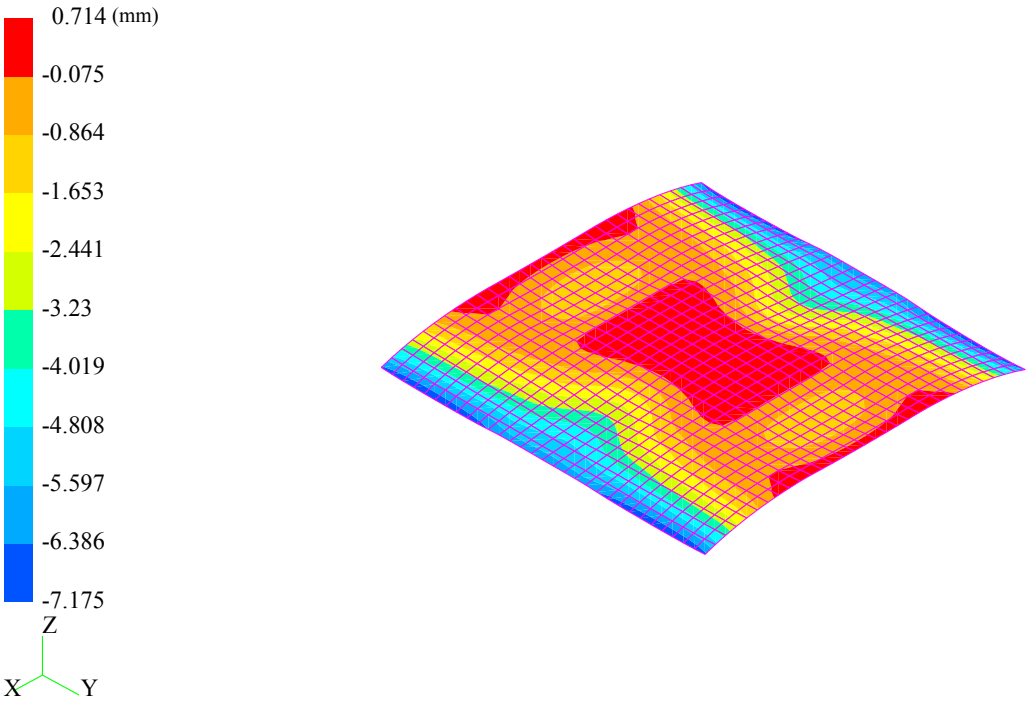


Figure 10: Final stable configuration of the compound surface of test case 2. The contours indicate positive displacement in the z-axis.

The instability of the intermediate states results from the strong interactions between connected elements. When a bistable element is actuated from the initial stable state, its curved edge will no longer be connected with the adjacent symmetric composite having a fibre direction perpendicular to this edge, which therefore has a relatively low stiffness. Instead the curved edge

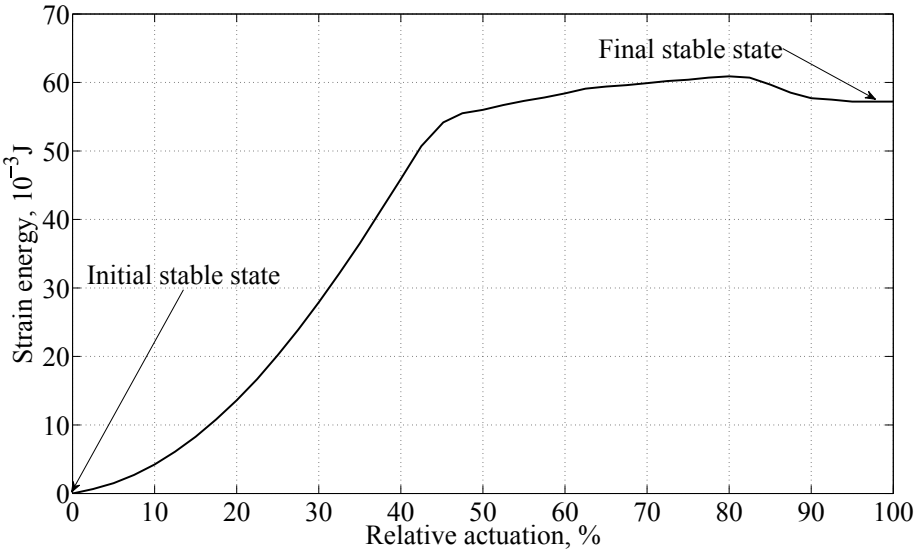
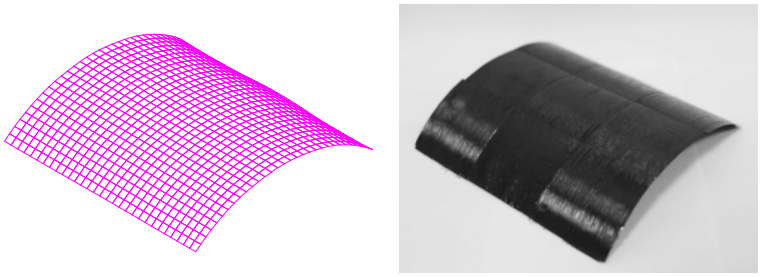


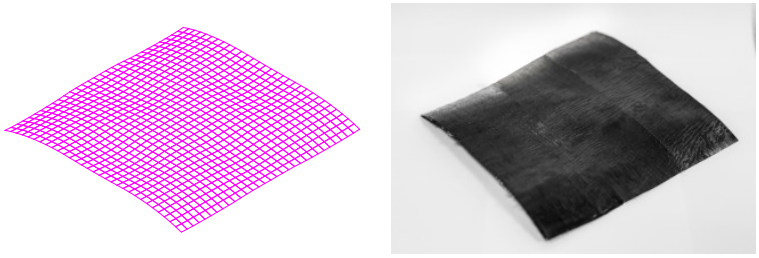
Figure 11: Strain energy vs. relative actuation percentage plots for the compound surface of test case 2 actuated from the initial stable state to the final stable state

is now linked to a symmetric element with fibres parallel to this linking edge. In this case the relative stiffness of the connnection is greater and significant strain energy is imparted to the bistable element leading to a reduction in curvature. If only one edge of the bistable element is connected with a monostable element, like the model investigated by Mattioni (2008), the bistability of this element is retained, but in this case, not only the curved edge of the bistable element but also one of the straight edges of the actuated bistable element will be subjected to imposed strain energy. The FE results indicate that the imparted energy is sufficient to overcome the actuation energy of the bistable element. Consequently, the bistable element snaps back and no new stable intermediate configurations can be achieved.

If all the bistable elements are actuated together, the strain energy imparted to the straight edge of the bistable elements will reduce and the compound surface can reach a second energy minimum. Thus, the surface of test case 2 is also bistable. Fig. 12 compares the stable configurations of the manufactured compound surface of test case 2 with the FEA results. Two stable states are found and similar shapes are exhibited.



(a) Initial stable state



(b) Second stable state

Figure 12: Two stable configurations of a physical model of the tessellated surface of test case 2 and the corresponding FEA results

4. Tessellated bistable composite shells with a monostable central element

As the two introduced composite tessellated surface cases cannot exhibit more than bistability, an alternative strategy is considered. The central elements of the tessellated surfaces are replaced by a symmetric composite laminate [0/0]. Since this laminate exhibits a flat shape at room temperature, the reduction in shape difference between the central element and its adjacent elements may reduce the interaction and lead the intermediate states to become stable.

Fig. 13 demonstrates the initial stable configuration of the surface of test case 1 with a monostable central element after curing. Due to the mismatch of the deformed shapes of two different types of bistable elements, the initial stable state of this surface still presents a undulating shape. The surface is in a configuration denoted

$$\begin{matrix} 0 & \bar{1} & 0 \\ \bar{1} & s & \bar{1} \\ 0 & \bar{1} & 0 \end{matrix} .$$

It is clear that larger out-of-plane displacement is achieved by using a monostable central element. However, this change does not bring more stable states

to this surface. To achieve another stable configuration, all the bistable elements have to be actuated. Fig. 14 shows the other stable shape of this tessellated surface: this surface is still bistable.

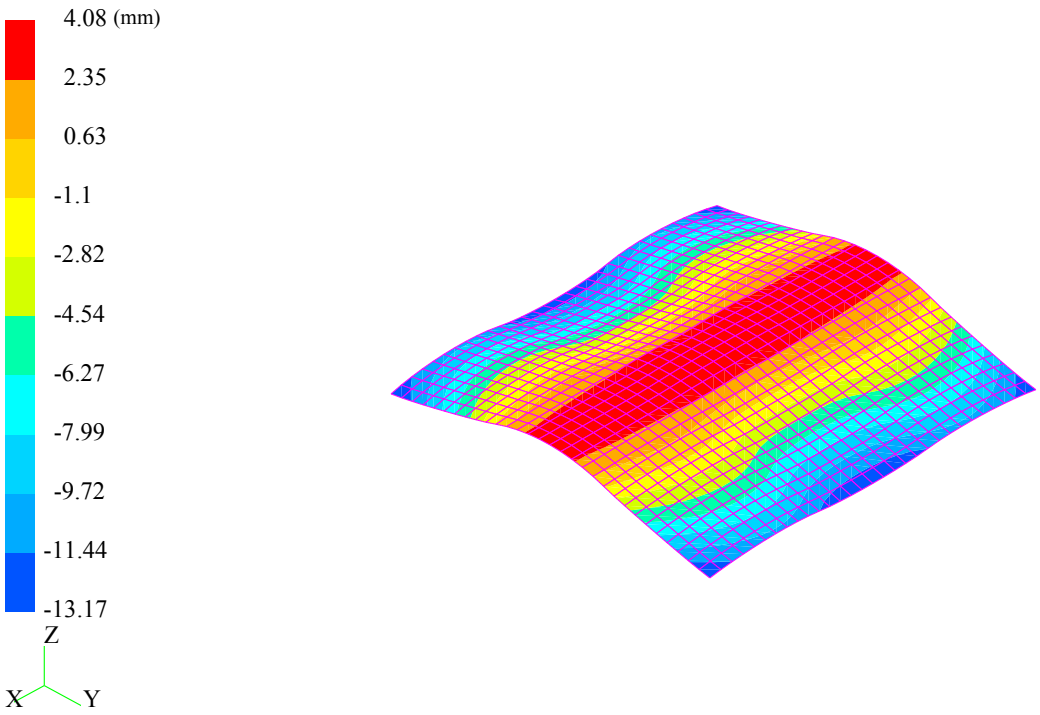


Figure 13: First stable configuration of tessellated surface of test case 1 with a monostable central element. The contours indicate positive displacement in the z-axis.

The results of coupled bistable shells with opposite layups can be used to interpret the instability of the intermediate states of this compound surface. When two bistable elements with opposite layups are connected by the curved edges, the strong mutual interaction will lead them to being unstable. Therefore, to reach a stable state, all these coupled edges of this tessellated surface have to ensure one or both of the edges are originally straight. There are only two configurations satisfying this requirement, i.e.

$$\begin{matrix} 0 & \bar{1} & 0 \\ \bar{1} & s & \bar{1} \\ 0 & \bar{1} & 0 \end{matrix} \quad \text{and} \quad \begin{matrix} 1 & \bar{0} & 1 \\ \bar{0} & s & \bar{0} \\ 1 & \bar{0} & 1 \end{matrix} .$$

This modified tessellated surface of test case 1 is manufactured. The experimental results also show the surface is bistable. The stable shapes are shown in Fig. 15.

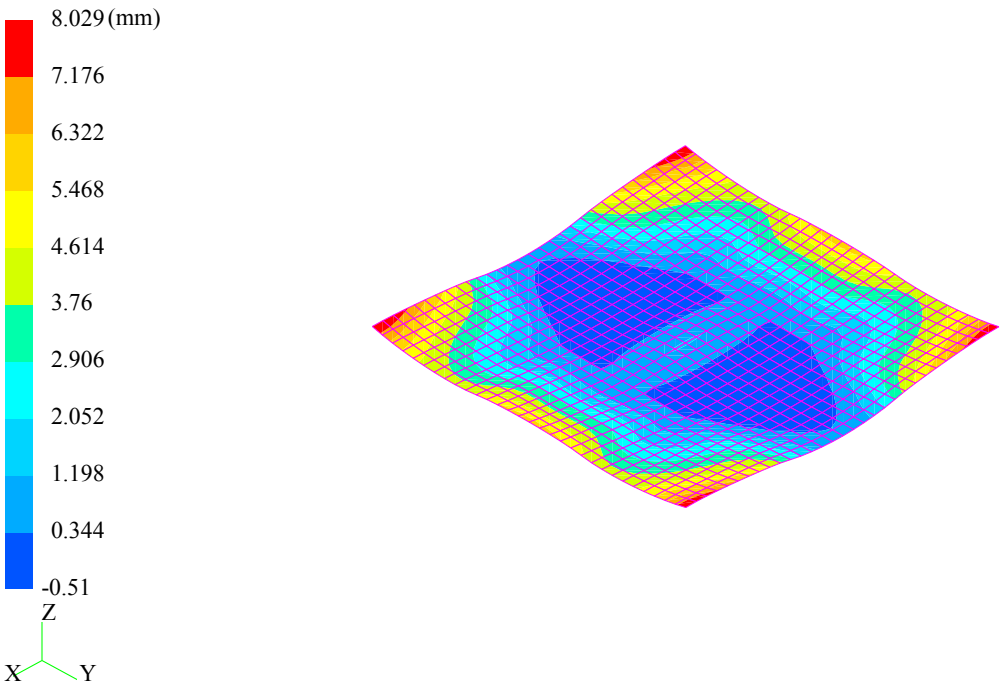
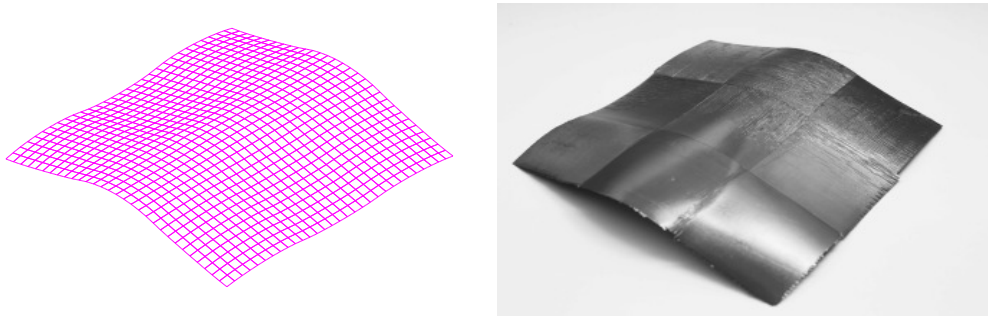
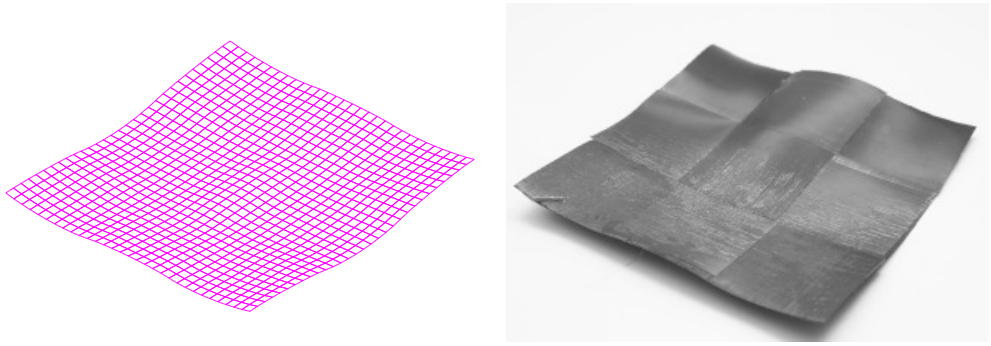


Figure 14: Second stable configuration of tessellated surface of test case 1 with a monostable central element. The contours indicate positive displacement in the z-axis.



(a) Initial stable state



(b) Second stable state

Figure 15: Two stable configurations of a physical model of the tessellated surface of test case 1 with a monostable central element and the corresponding FEA results

When the monostable laminate [0/0] is used as the central element of the test case 2 surface, all the elements directly connected with the central element are monostable composite shells. This design avoids the central element generating considerable displacement mismatches with its adjacent elements. This in turn helps the compound surface to achieve intermediate stable states.

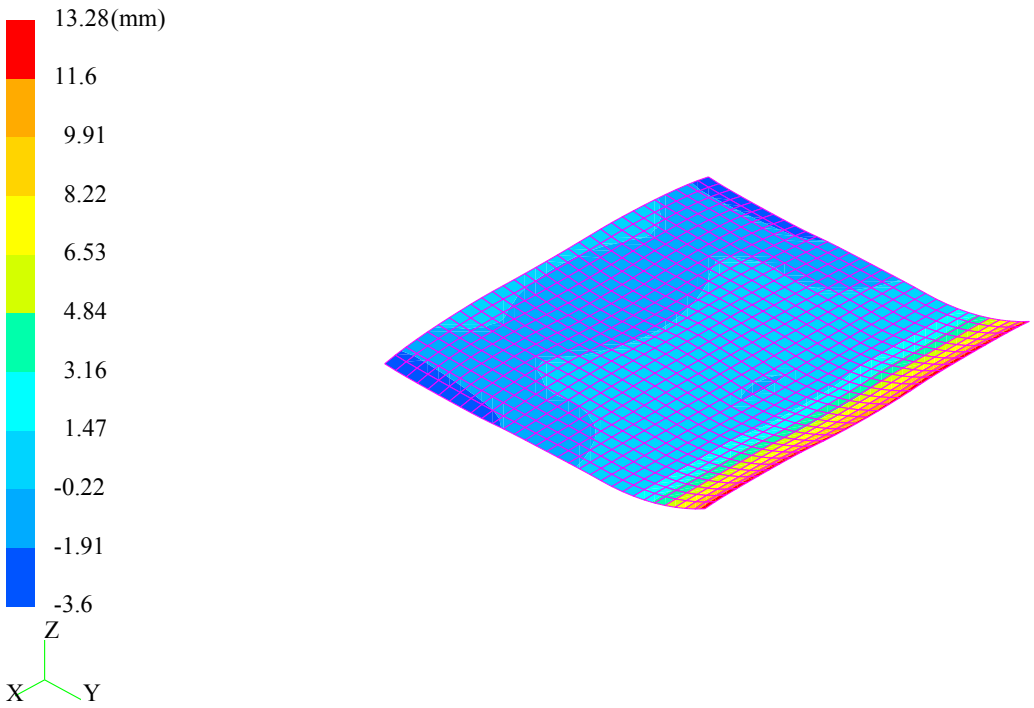


Figure 16: First intermediate stable configuration of tessellated surface of test case 2 with a monostable composite central element. The contours indicate positive displacement in the z-axis.

The FE results show that the compound surface with a monostable central element can present two stable intermediate states as shown in Figs. 16 and 17. They are

$$\begin{matrix} 1 & s & 1 \\ s & s & s \\ 0 & s & 0 \end{matrix} \quad \text{and} \quad \begin{matrix} 1 & s & 0 \\ s & s & s \\ 1 & s & 0 \end{matrix}.$$

The results also imply the stability of other two symmetric intermediate states. i.e.

$$\begin{matrix} 0 & s & 0 \\ s & s & s \\ 1 & s & 1 \end{matrix} \quad \text{and} \quad \begin{matrix} 0 & s & 1 \\ s & s & s \\ 0 & s & 1 \end{matrix}.$$

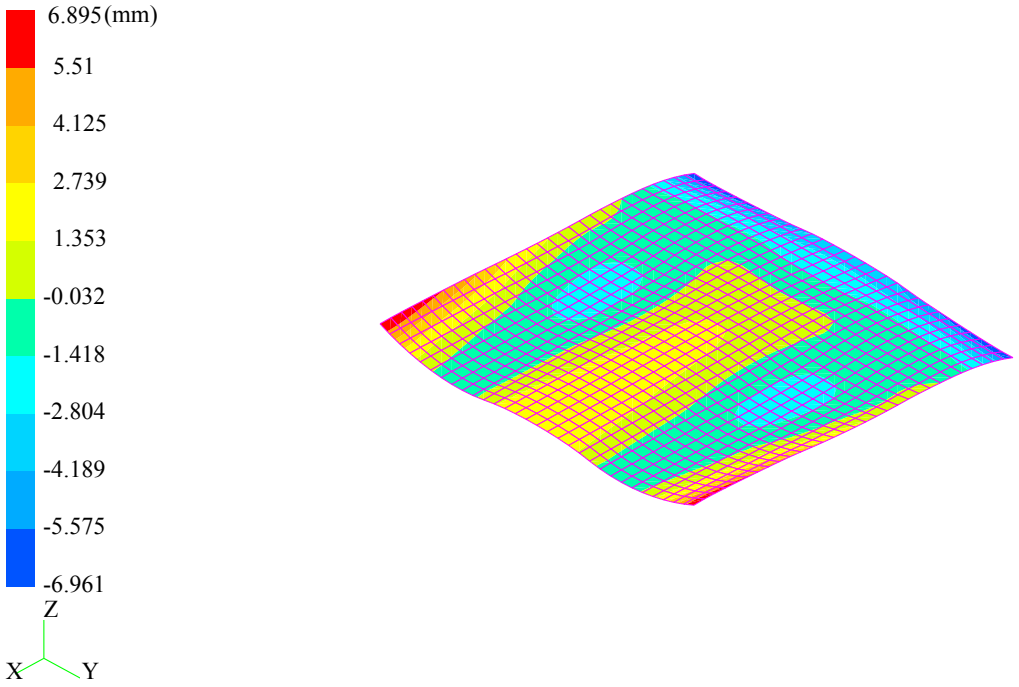


Figure 17: Second intermediate stable configuration of tessellated surface of test case 2 with a monostable composite central element. The contours indicate positive displacement in the z-axis.

The compound surface of test case 2 with a monostable central element can therefore demonstrate six stable configurations.

To show the influence of using different central elements on the multistability of the tessellated surface, a comparative energy graph is plotted in Fig. 18. Two different tessellated surfaces based on test case 2 are actuated from a primary stable state to an intermediate state. For the tessellated surface with a monostable central element, a local energy minimum is demonstrated at the intermediate state. In contrast, the intermediate stable state disappears when the surface uses a bistable central element.

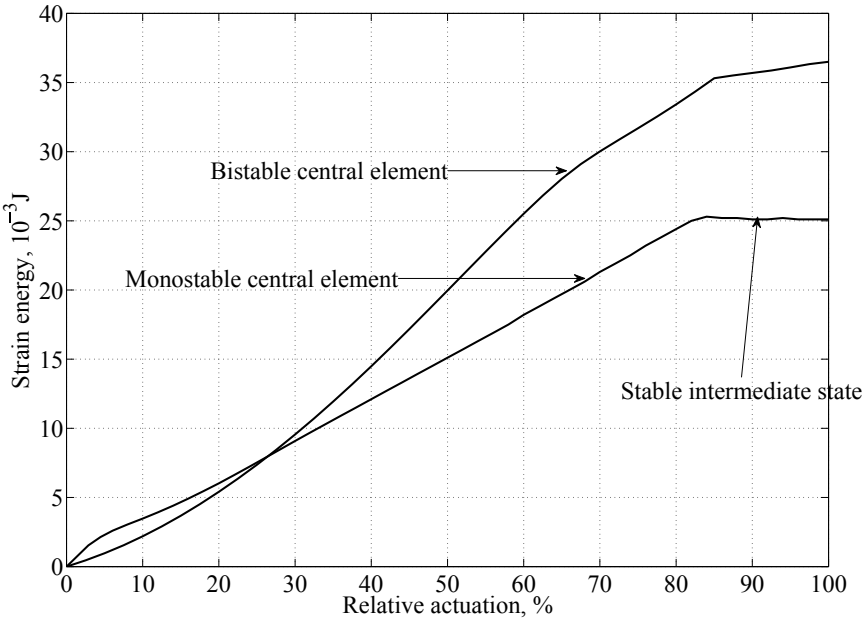


Figure 18: Strain energy vs. relative actuation percentage plots for tessellated surfaces of test case 2 with different central elements

Although the compound surface with a monostable composite central element shows a maximum of six discrete stable configurations, this multistable behaviour cannot be maintained when the 3×3 compound surface is used as the fundamental unit of a larger tessellated surface. As shown in Fig. 18, the actuation energy, i.e. the energy necessary to exit the energy well, of the intermediate stable state is relatively low and indicates a weakly-stable configuration. It should be noted that all the bistable elements of the compound surface, which are the keys of possessing high degree of multistability, are located at the corner region of the surface with only two edges clamped. When the tessellated surface is connected with other repeated tessellated surfaces,

the behaviour of these bistable elements are affected by more elements. Thus, stronger interactions will easily trigger the tessellated surface from the intermediate state to a more stable primary stable state.

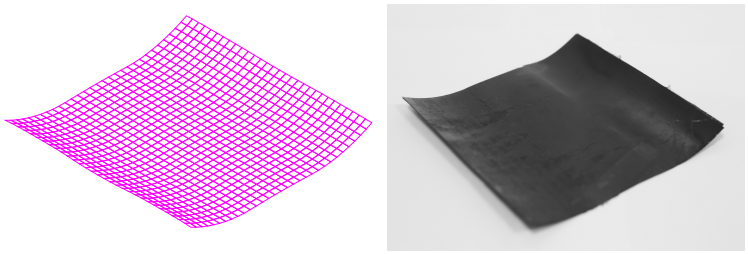
The high degree of multistability of this tessellated surface is verified experimentally. Fig. 19 illustrates the stable configurations of the manufactured tessellated surface and the FEA results. Due to symmetry, only two intermediate stable states are presented. The manufactured tessellated surface demonstrates six stable shapes. The physical model shows good qualitative agreement with the predicted results. Some discrepancies are observed around one corner region, especially in Fig. 19d. Due to geometric imperfections introduced during manufacture, the layup of one bistable element is not perfectly [0/90] and consequently a small amount of twisting curvature is introduced.

5. Extendable tessellated surfaces

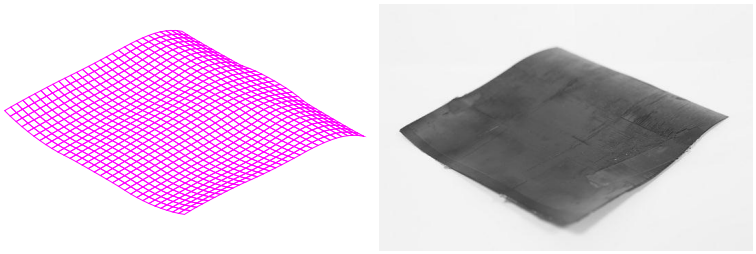
The overarching aim of this research is to achieve an infinite tessellated surface in which fundamental sub-elements can present isolated multistability. The key to achieving an infinite multistable tessellated surface is the fact that a bistable composite element can maintain its bistability when it is connected with eight surrounding elements. The above analysis has demonstrated that a square unsymmetric composite shell is no longer bistable when it is surrounded by other bistable elements. This is because the edge interaction is too strong when the adjacent elements are in different stable states.

To maintain the bistability of an unsymmetric composite shell, another tessellated surface is introduced. As shown in Fig. 20, a bistable square element is connected with eight monostable composite elements. To minimise the interaction between the bistable element and the surrounding elements, the monostable elements only have one layer. If the bistable element can maintain its bistability in this test case, the tessellated surface may form the fundamental unit of a larger tessellated surface. If the bistable tessellated surface can reach a stable state different from other surrounding tessellated surfaces, we can conclude a repeatable bistable tessellated surface is achieved and an infinite multistable tessellated surface can be built.

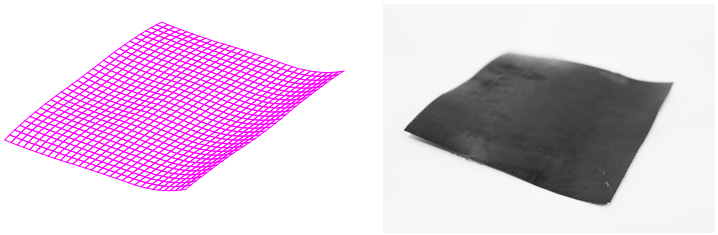
The multistability of the tessellated surface consisting of one bistable composite element and eight monostable composite elements is investigated by FEA. Fig. 21a shows the initial stable shape of the tessellated surface after thermal curing. The central unsymmetric element reaches a curved stable shape and causes the deformation of the symmetric composite elements, especially the two elements connected to the curved edges of the central bistable element. To investigate whether the bistability of the central unsymmetric element vanishes due to the full fixation, the central bistable element is actu-



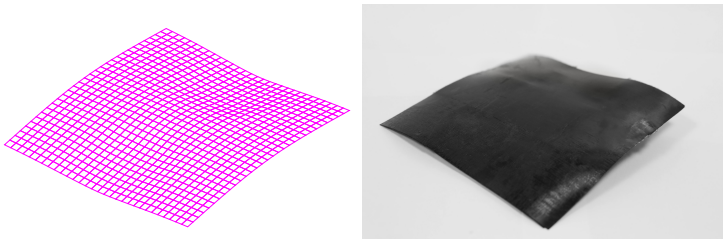
(a) Initial primary stable state



(b) First intermediate stable state



(c) Second intermediate stable state



(d) Final primary stable state

Figure 19: Four stable configurations of the tessellated surface of a physical model of test case 2 with a monostable central element and the corresponding FEA results

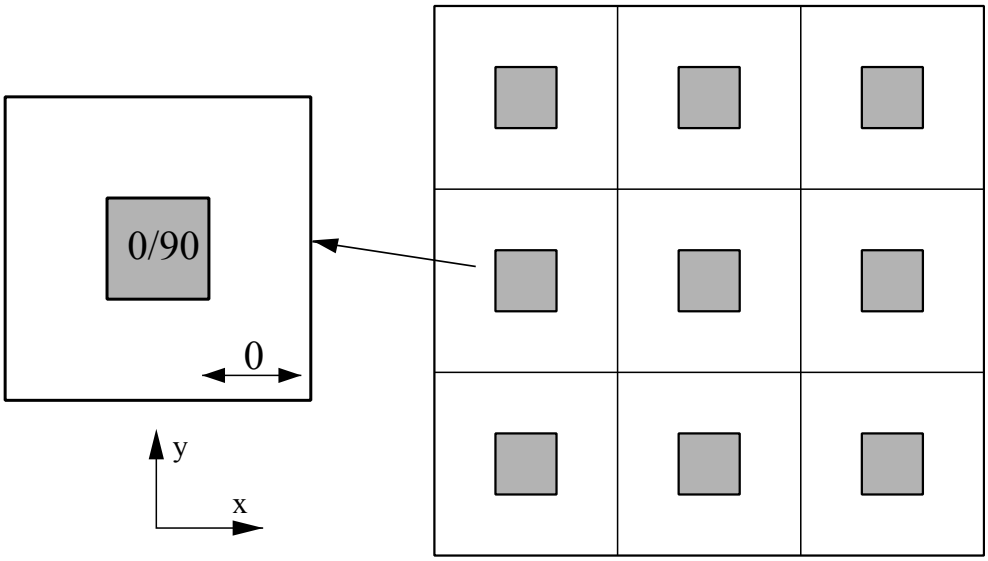
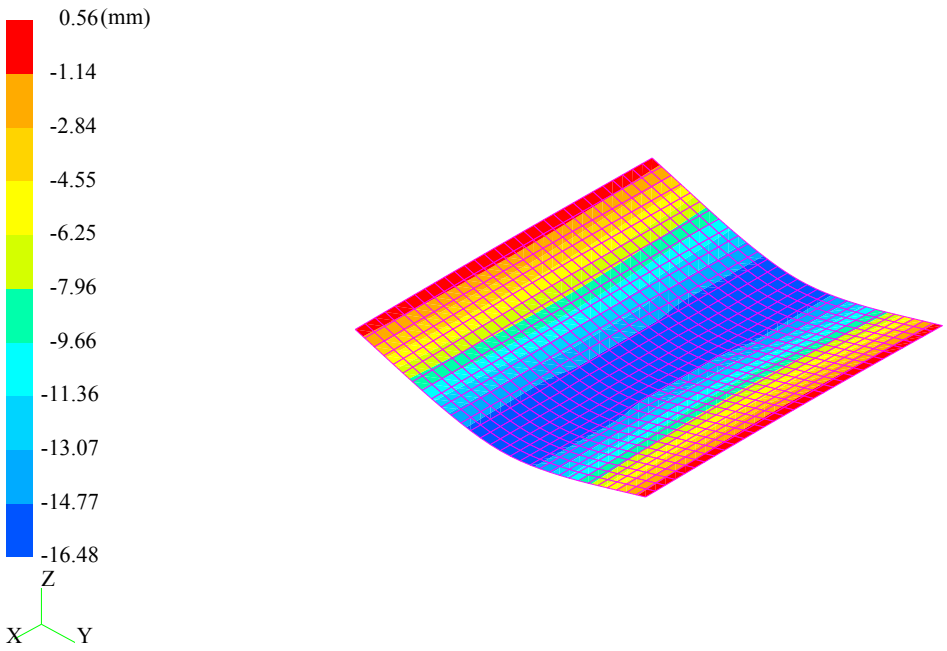


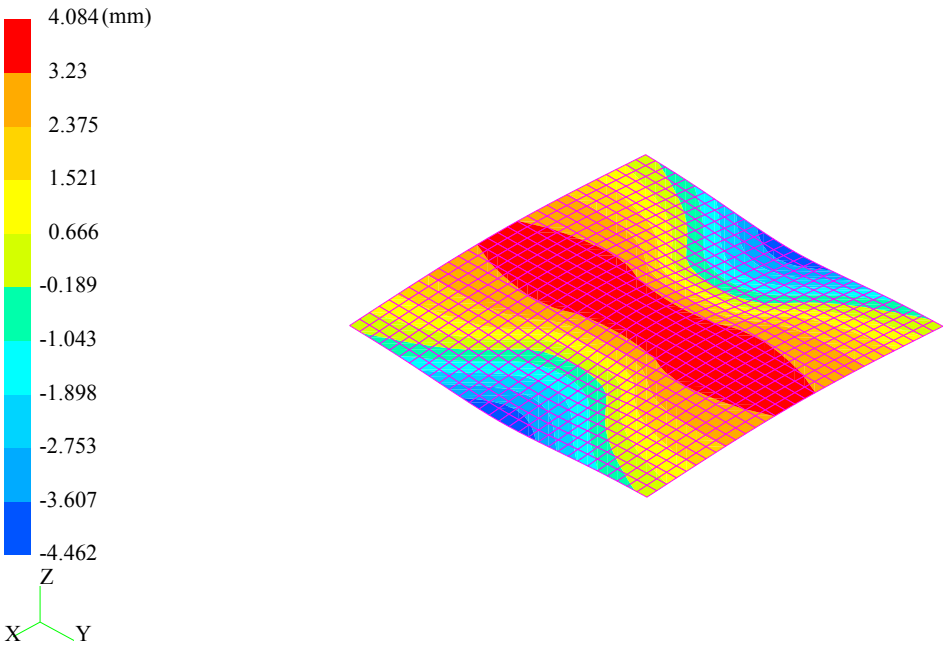
Figure 20: A compound surface composed of a bistable square element surrounded by monostable elements and a 3×3 tessellation of this surface

ated and the whole surface reaches another stable configuration successfully as shown in Fig. 21b. However, the out-of-plane deformation of the central element is significantly affected by the connected monostable elements. This is because the fiber direction of monostable elements is parallel to the curved edges of the central bistable element in this stable shape. Stronger interaction between the curved element and the originally flat monostable elements is generated. The asymmetric bistability of this tessellated surface is clearly demonstrated by the strain energy graph shown in Fig. 22. Fig. 23 compares the FEA results with the behaviour of a physical model. It is clear the manufactured composite shell also demonstrates bistability.

Having demonstrated the bistability of this tessellated surface, the next step is to repeat this surface to form a larger tessellated surface as shown in Fig. 20. To verify the isolated bistability of this surface, the central tessellated surface is controlled to deform into the second stable configurations and the rest tessellated surfaces are in the preferred stable configurations. In this case, the interaction between the central tessellated surface and the surrounding surfaces is maximised and the actuation energy of the central surface is relatively low. If this configuration is stable, we can confirm that the bistable elements in this tessellated surface possess isolated bistability. According to the results from FEA, the surface cannot reach a energy equilibrium at this configuration. The central tessellated surface snaps back to the preferred stable configuration automatically by the influence of the connected surfaces.



(a) Initial stable state



(b) Second stable state

Figure 21: Two stable configurations of the tessellated surface composed of one central bistable elements and eight monostable composite elements. The contours indicate positive displacement in the z-axis.

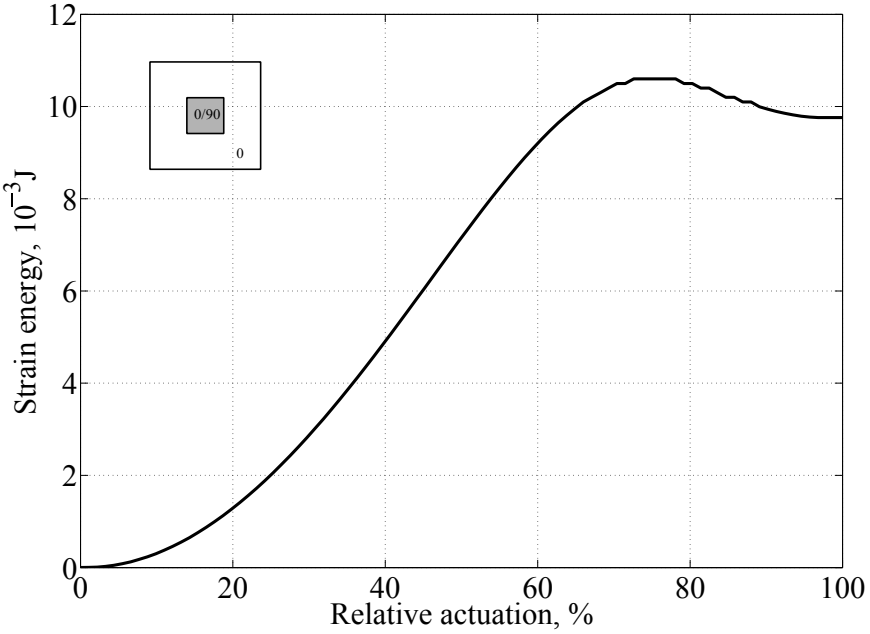
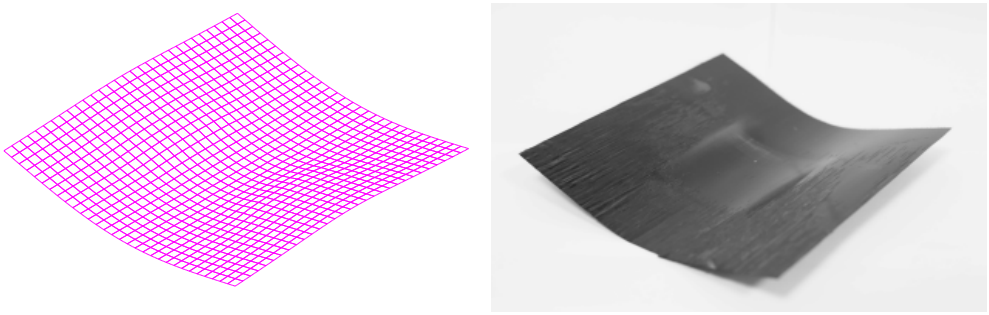
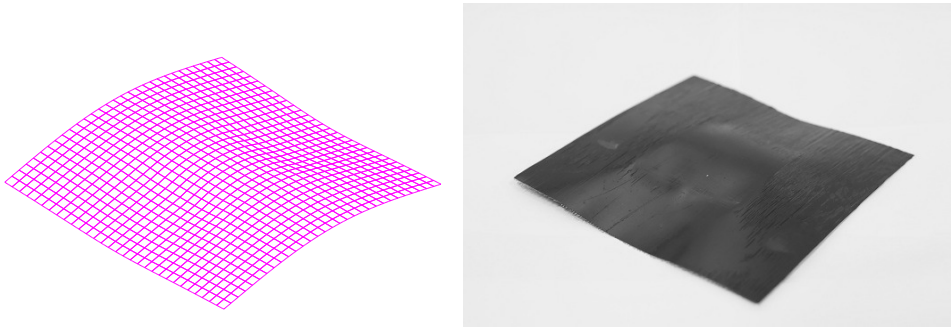


Figure 22: Strain energy vs. relative actuation percentage plots for the tessellated surface composed of one central bistable elements and eight monostable composite elements



(a) Initial stable state



(b) Second stable state

Figure 23: Experimental results and FEA results of two stable configurations of the tessellated surface composed of one central bistable elements and eight monostable composite elements

To help the basic tessellated surface to maintain its bistability when it is connected with repeated surfaces, the actuation energy of the less preferred stable state needs to be maximised. This means the asymmetric bistability of the basic tessellated surface has to be tailored.

A refined model of one bistable composite element connected with eight monostable elements is designed. An isotropic material is used to replace the one-layer composite laminate. The thickness of the isotropic material is the same as the thickness of one layer laminate. To investigate the influence of the stiffness of the isotropic materials on the multistability of the compound surface, the Young's modulus of the material is set to be two different values, 50% and 100% of the Young's modulus of the composite material in the fibre direction. Fig. 24 demonstrates the potential energy curves of compound surfaces composed of different isotropic materials during the actuation. All these surfaces exhibit symmetric bistability. Fig. 25 shows the two stable configurations of one tessellated surface composed of one bistable central element and eight virtual isotropic elements. Two similar configurations of these state stables demonstrate the symmetric bistability. With the Young's modulus increasing, the actuation energy reduces. This is because stiffer material can reduce the out-of-plane displacement of the central bistable element. Consequently, the tessellated surface becomes less stable.

Larger tessellated surfaces are built by connecting nine identical tessellated surfaces composed of a central bistable element and isotropic elements. After thermal curing, the surface is deformed into the primary stable state in which the nine fundamental tessellated surfaces are all in the same stable state. Then the central tessellated surface is actuated following the previously-defined displacement-controlled procedure. Fig. 26 shows the strain energy graph of this actuation process. For the surface using stiffer isotropic material, the central bistable tessellated surface cannot be actuated in isolation. However, the surface using low Young's modulus isotropic material can achieve a stable intermediate state. Fig. 27 illustrates the two stable configurations of this compound surface. The central tessellated surface is in a different stable state from the remaining tessellated surfaces and crucially the resulting distortion is contained within the surrounding eight elements. This means that each bistable unit is effectively isolated from the others and therefore it indicates this bistable tessellated surface is infinitely extendable. This model successfully demonstrates that it is possible to achieve a continuous tessellated surface which possesses n bistable elements can present a maximum 2^n stable states.

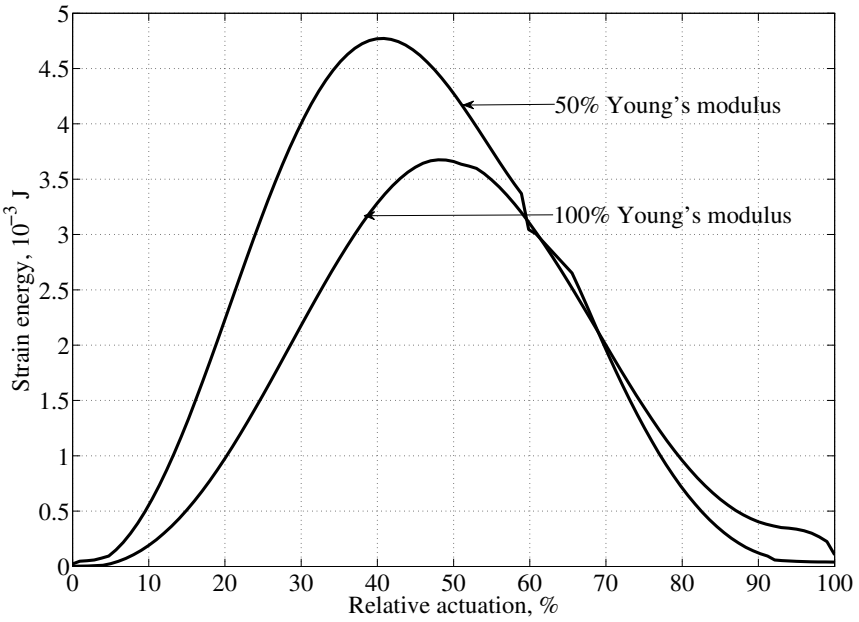
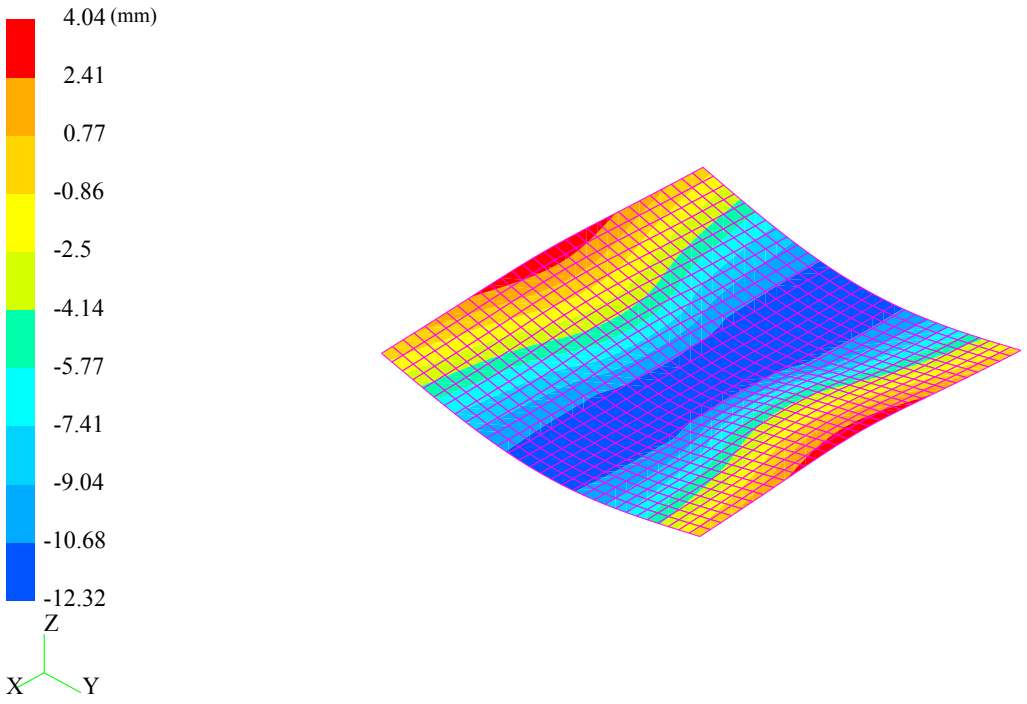
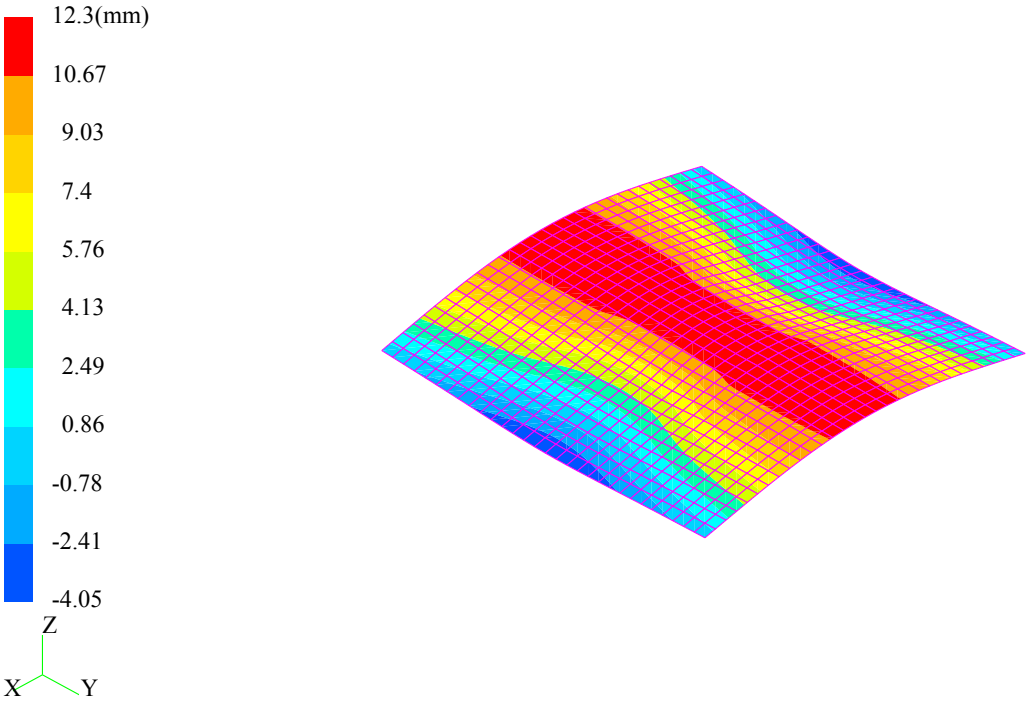


Figure 24: Strain energy vs. relative actuation percentage plots for the compound surfaces composed of one central bistable element surrounded by eight isotropic elements of varying Young's modulus



(a) First stable state



(b) Second stable state

Figure 25: Two stable configurations of a tessellated surface composed of one central bistable elements and eight isotropic elements at 50% Young's modulus. The contours indicate positive displacement in the z-axis.

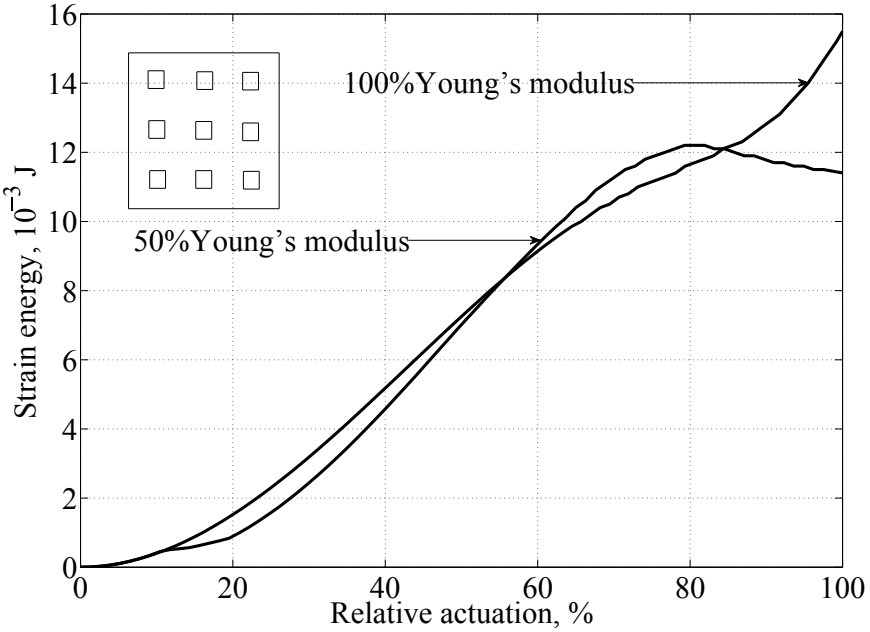
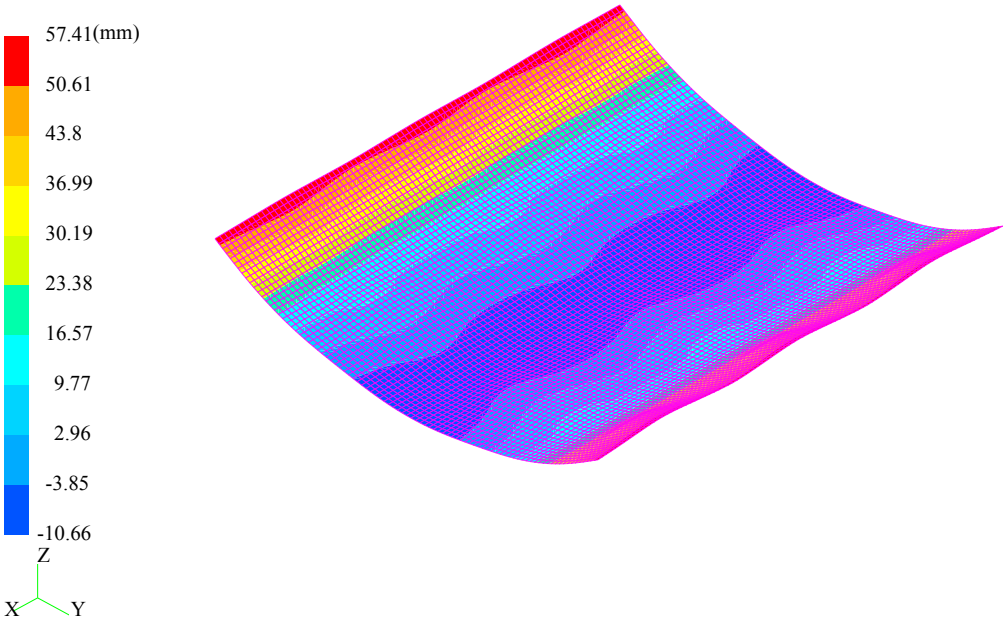
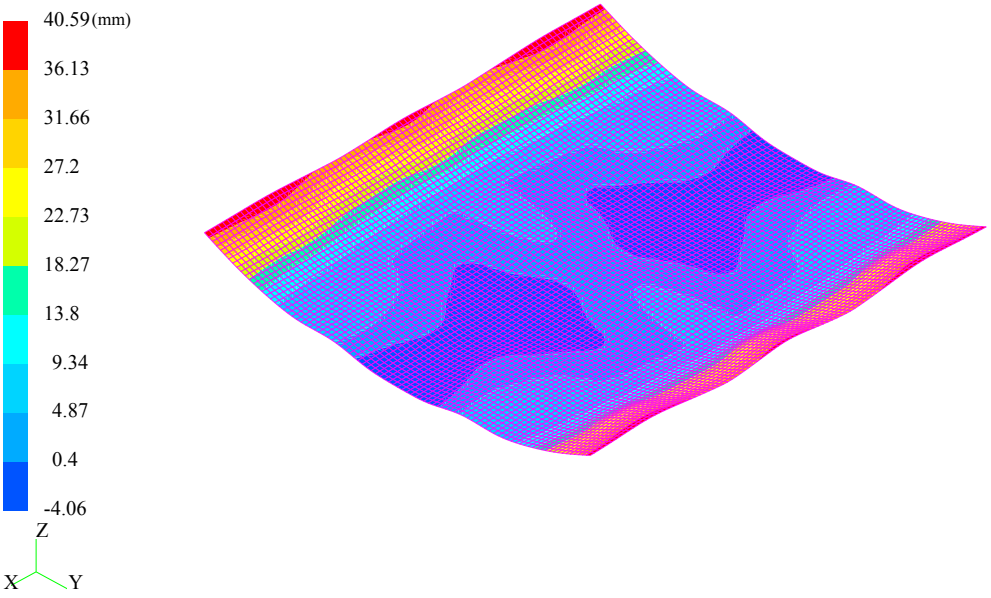


Figure 26: Strain energy vs. relative actuation percentage plots for tessellated surfaces composed of nine central bistable elements and isotropic elements with varying Young's modulus



(a) Primary stable state



(b) Intermediate stable state

Figure 27: Two stable configurations of a tessellated surface composed of nine bistable composite elements and isotropic elements. The contours indicate positive displacement in the z-axis.

6. Conclusions

To develop highly multistable three-dimensional surface, tessellated surfaces composed of 3×3 distinct composite elements have been designed in this paper. Before the investigation of the tessellated surfaces, coupled composite shells with opposite layups are studied first as this forms a fundamental unit. It is shown that this compound surface cannot be stable when two cured edges are connected, because strong edge interaction will lead one element to snap through.

The achieved understanding of the behaviour coupled composite shells assists the study of the more complex tessellated composite surfaces. The multistable behaviour of different tessellated composite surfaces are summarised as follows in order of increasing levels of adaptability:

- a tessellated surface denoted test case 1 — defined in Fig. 4 — composed of bistable composite elements with opposite layups, exhibits symmetric bistability and relatively small out-of-plane surface displacements;
- a tessellated surface denoted test case 2 — defined in Fig. 10 — composed of five bistable composite elements and four monostable bistable elements exhibits asymmetric bistability;
- a modification to the first test case of tessellated surface, in which the central element is replaced with a monostable composite element, leads to larger out-of-plane displacements, but no increase in the number of stable states — the surface remains bistable;
- a modification to the second test case of tessellated surface, in which the central element is replaced by a monostable composite element, exhibits a maximum of six stable shapes.

The strong interactions between adjacent elements determine the multistable behaviour of tessellated surfaces. The multistable behaviour of these tessellated surfaces indicates that connecting monostable composite elements with bistable elements can reduce the interactions and makes possible highly multistable tessellated surfaces.

These tessellated surface models inspire another multistable compound surface design which can exhibit theoretically maximum number of stable shapes. The fundamental unit is a tessellated surface composed of a central bistable composite shell and eight surrounding monostable shells. By tailoring the mechanical properties of the monostable elements, such surfaces consisting of n bistable elements are shown to be able to exhibit the theoretical maximum of 2^n discrete stable states.

References

Cui Y., Santer M., Highly multistable composite surfaces, Composite Structures, 124 (2015), pp.44-54.

Hyer M. W., Some observations on the cured shape of thin unsymmetric laminates, Journal of Composite Materials, 15 (1981), pp.175-94.

Hyer M. W., The room-temperature shapes of four-layer unsymmetric cross-ply laminates, Journal of Composite Materials, 16 (4)(1982), pp.318-40.

Dang J., Tang Y., Calculation of the room-temperature shapes of unsymmetric laminates, Proceedings of the International Symposiium on Composite Materials and Structures. 1986, Lancaster, PA, USA, pp.201-206.

Jun W. J., Hong C. S., Cured shape of unsymmetric laminates with arbitrary lay-up angles, Journal of Reinforced Plastics and Composites, 11 (12)(1992), pp.1352-1366.

Peeters L. J. B., Powell P. C., Warnet L., Thermally-induced shapes of unsymmetric laminates, Journal of Composite Materials, 30 (5)(1996), pp.603-26.

Dano M. L., Hyer M. W., Room-temperature shape of general unsymmetric laminates, Proceedings of the 1996 11th Technical Conference of the American Society for Composites, October 7-9,1996. Virginia Polytechnic Inst and State, Univ, Blacksburg, United States, Technomic Publ Co Inc, Atlanta, GA, USA, pp. 100-10.

Etches J., Potter K., Weaver P., Bond I., Environmental effects on thermally induced multistability in unsymmetric composite laminates, Composites Part A: Applied Science and Manufacturing, 40 (8)(2009), pp.1240-1247.

Mattioni F., Weaver P. M., Potter K. D., Friswell M. I., Analysis of thermally induced multistable composite, International Journal of Solids and Structures 45 (2)(2008), pp.657-75.

Arrieta A., Kuder I., Waeber T., Ermanni P., Varible stiffness characteristics of embeddable multi-stable composites, Composite Science and Technology, 97 (2014), pp.12-18.

Dai F., Li H., Du S., A multi-stable lattice structure and its snapthrough behavior among multiple states, Composite Structures, 99 (2013), pp.56-63.

Hyer M. W.,Calculations of the room-temperature shapes of unsymmetric laminates, Journal of Composite Materials, 15 (1981), pp.296-310.

Potter, K.D., Weaver, P.M., A concept for the generation of out-of-plane distortion from tailored frp laminates, (2004) Composites Part A: Applied Science and Manufacturing, 35 (12), pp. 1353-1361.

Eckstein, E., Weaver, P.M., Developments in Morphing Composites, AIAA Paper No. AIAA 2012-1378, Proceedings of the 53rd AIAA/ASME/ASCE/AHS/ASC Structures, Structural Dynamics, and Materials Conference. Honolulu, HI, Jan-16, 2012

Panesar, A.S., Weaver, P.M., Optimisation of blended bistable laminates for a morphing flap, Composite Structures, 94 (10), pp. 3092-3105, 2012